scientific reports

Check for updates

OPEN

Distinct gut microbial signature and altered short chain fatty acid metabolism at disease onset in a rat preclinical model of superimposed preeclampsia

Moumen M. Alhasan[1], María S. Landa[2,3], Silvia I. García[2,3,4], Roman G. Gerlach[5], Hani Harb[6], Fabian B. Fahlbusch[7], Melanie L. Conrad[1,7,9] & Gabriela Barrientos[4,8,9]✉

Chronic hypertension is an increasingly prevalent condition that constitutes a risk factor for superimposed preeclampsia during pregnancy. In this study, we assessed the gut microbiome in a rat model of superimposed preeclampsia to characterize the microbial signature associated with defective placentation processes identified at the preclinical disease stage. The blood pressure profile, renal function parameters and fetal phenotype were evaluated in pregnant Stroke-prone Spontaneously Hypertensive Rats (SHRSP) and their normotensive controls. On gestation day (GD)14, feces were collected and gut microbiome composition and short-chain fatty acid concentrations were determined by 16S rRNA sequencing and gas chromatography respectively. At disease onset on GD14, the fecal gut microbiome of SHRSP showed a lower alpha diversity and significant differences in beta diversity when compared with control animals. In the feces, *Prevotella*, *Bifidobacterium*, *Parasutterella* and *Roseburia* were enriched in SHRSP pregnancies compared to controls, showing a strong correlation with clinical parameters. Bacteria from the families *Ruminococcaceae*, *Oscillospiraceae* and the genera *Blautia* and *Faecalibacterium* were depleted. Considering short-chain fatty acids, acetate, propionate and valerate were increased in the SHRSP model, showing a strong positive correlation with the relative abundance of enriched taxa. We show that on GD14, at the asymptomatic SPE onset stage, pregnant SHRSP display a distinct gut microbiome signature and altered short chain fatty acid metabolism compared to control animals.

Chronic hypertension constitutes an increasingly prevalent complication in pregnancy, affecting up to 5% of pregnancies and representing the main maternal risk factor for the development of preeclampsia (PE)[1]. Superimposed PE (SPE) occurs in 20–40% of women with chronic hypertension, and after adjusting for confounding factors, the risk of preterm SPE is 5 to 6 times higher in women with a preexisting hypertensive condition. Development of SPE is associated with a higher incidence of adverse maternal and perinatal outcomes, including preterm birth, delivery of small-for-gestational-age neonates and consequent admission to the neonatal intensive care unit[2,3]. Diagnosis of SPE is still challenging, since in chronic hypertension the

[1]Institute of Microbiology, Infectious Diseases and Immunology, Charité-Universitätsmedizin Berlin, Corporate Member of Freie Universität Berlin, Humboldt-Universität Zu Berlin, Berlin Institute of Health, Berlin, Germany. [2]Facultad de Medicina, Instituto de Investigaciones Médicas Alfredo Lanari, Universidad de Buenos Aires (UBA), Ciudad Autónoma de Buenos Aires, Argentina. [3]Laboratorio de Cardiología Molecular, Instituto de Investigaciones Médicas (IDIM), Universidad de Buenos Aires (UBA), Consejo Nacional de Investigaciones Científicas y Técnicas (CONICET), Ciudad Autónoma de Buenos Aires, Argentina. [4]Laboratorio de Medicina Experimental, Hospital Alemán, Av. Pueyrredón 1640, C1118AAT Ciudad Autónoma de Buenos Aires, Argentina. [5]Institute of Clinical Microbiology, Immunology and Hygiene, University Hospital of Erlangen and Friedrich-Alexander-University (FAU) Erlangen-Nuremberg, Erlangen, Germany. [6]Institute for Medical Microbiology and Virology, Medical Faculty, TU Dresden, Dresden, Germany. [7]Neonatology and Pediatric Intensive Care, Faculty of Medicine, University of Augsburg, 86156 Augsburg, Germany. [8]Consejo Nacional de Investigaciones Científicas y Técnicas (CONICET), Buenos Aires, Argentina. [9]Melanie L. Conrad and Gabriela Barrientos contributed equally. ✉email: gbarrientos@hospitalaleman.com

clinical signs traditionally considered as assessment criteria can often predate the pregnancy. Therefore, there is a growing need to identify biomarkers for screening and diagnosis and to aid in the stratification of risk in women with chronic hypertension.

Animal models are instrumental to investigate causative associations in PE pathogenesis, and to evaluate possible strategies for diagnosis and intervention. However, few models available thus far are representative of the pathogenesis of SPE. Our previous studies demonstrated that the Stroke-prone Spontaneously Hypertensive Rat (SHRSP), a well-studied model of chronic hypertension, develops a SPE phenotype during pregnancy with distinct placental, maternal and fetal features[4]. In this model, disease onset is characterized by a preclinical stage occurring mid-pregnancy, comprising placental vascular alterations, impaired trophoblast invasion and activation of oxidative stress pathways[4,5], which ultimately result in placental dysfunction and an asymmetric fetal growth restriction phenotype of the offspring. On the maternal side, the clinical syndrome is fully established towards term, with impaired blood pressure control and signs of renal compromise including decreased urine output, impaired filtration and eventual proteinuria[4,6].

In the past decades, an emerging concept is that the gut microbiome acts as a key determinant of health and disease[7]. Pathogenic alterations in the composition and function of the gut microbiome—known as dysbiosis—have been linked to the development of cardiometabolic disorders including chronic hypertension[8–10]. Compositional microbiota variations are reflected by measurements of alpha diversity (number of taxa), beta diversity (differences between groups) and differences in the relative abundance of bacterial taxa. In particular, the relationship between the two dominant phyla, expressed as the *Firmicutes*:*Bacteroidetes* ratio, has been associated with different pathological conditions and is considered a marker of gut dysbiosis[11]. The association of gut microbiome alterations and hypertensive conditions may be driven by microbial-derived metabolites such as short-chain fatty acids (SCFAs), which can participate in several mechanisms relevant to blood pressure regulation, including vasodilation, renal sodium/potassium regulation, and immune modulation[12,13]. Accordingly, recent studies show that compared to its normotensive control strain, the SHRSP display a distinct gut bacterial community structure already in the pre-hypertensive stage, as early as four weeks of age[14]. While cross-fostering and microbiota transplant experiments have demonstrated that gut dysbiosis in the SHRSP has an underlying role in the development of hypertension[15,16], little is known on the specific bacterial taxa and mechanisms associated with different pathophysiological contexts in this model.

During pregnancy, the gut microbiome undergoes significant adaptive changes in bacterial composition in response to physiological processes of the host[17,18]. However, our knowledge on the impact of a pre-existing dysbiotic gut microbiome on these physiological adaptations is still limited. In an attempt to shed light on the contribution of gut dysbiosis to the development of SPE, the aim of this study was to characterize the microbial signature associated with disease onset in SHRSP pregnancies and its correlation with maternal signs.

Results

Description of the model and assessment of maternal signs at disease onset

We previously demonstrated that pregnant SHRSP represent a preclinical model of SPE with distinct placental, maternal and fetal features (Fig. 1a)[4,6]. During pregnancy, SHRSP spontaneously develop increased blood pressure, signs of renal compromise and asymmetric FGR[4]. These features develop as a result of impaired placentation with defective trophoblast invasion[4] and activation of placental cellular stress pathways[5,19]. To verify reproducibility of these findings, we established congenic timed pregnancies of control (WKY) or SHRSP animals and characterized disease progression by assessing maternal signs and fetal growth parameters. As shown in Fig. 1b, SHSRP showed a progressive worsening of the hypertensive condition towards term, displaying a significantly increased systolic blood pressure on GD14 (168.2 ± 16.7 vs.154.7 ± 10.2 mmHg, $p < 0.01$) compared to baseline records. Further analyses of urine samples collected on GD20 revealed a significant decrease of the creatinine clearance rate in SHRSP compared to controls (1.70 ± 0.08 vs. 1.32 ± 0.04 ml/min, $p > 0.01$, Fig. 1c left panel). Moreover, although no differences were observed in proteinuria (Fig. 1c, right panel), histological assessment of maternal kidneys demonstrated structural alterations (i.e., glomerular enlargement) and a significant decrease of podocin expression in SHRSP (Fig. 1d), indicative of glomerular damage. Morphometrical assessment of GD20 fetal specimens verified the FGR phenotype in SHRSP, as noted by the significantly decreased fetal weight compared to controls (1.98 ± 0.03 vs. 2.20 ± 0.04 g, $p > 0.0001$) and increased proportion of specimens with weight below the 10th percentile (Fig. 1e). Thus, we verified the SPE phenotype in SHRSP pregnancies[4,6], which manifests as a progressive worsening of the hypertensive condition starting on GD14 and is associated with defective vascular remodeling in the placental bed[4].

Next, to characterize the maternal phenotype at the onset of disease, we assessed several clinical parameters in pregnant females on GD14, shown in Fig. 2. Urine analysis revealed no differences in creatinine clearance or urinary protein levels, and a significant decrease of the urine output in SHRSP dams (Fig. 2a). Circulating levels of Flt-1 in SHRSP pregnancies, as measured by ELISA, did not differ from control pregnancies (Fig. 2b). Finally, assessment of the number of implantations showed no differences between control and SHRSP animals, nor did the mothers show any differences in weight gain on GD14 (Fig. 2c). In summary, SHRSP dams show increased systolic blood pressure and decreased urine output compared to controls on GD14. No other differences in clinical parameters were observed, indicating that GD14 (referred to as disease onset) represents an adequate timepoint to study the gut microbiome during the pre-clinical stage in this model.

Onset of disease in SHRSP is characterized by a distinct microbial signature and decreased diversity of the bacterial community

After characterizing maternal clinical parameters, we next examined the GD14 fecal microbiota to identify the specific microbial profile associated with disease onset in our model. 16S rRNA amplicon sequencing revealed marked differences in the SHRSP fecal microbiome as compared to controls. This was evidenced by a significantly

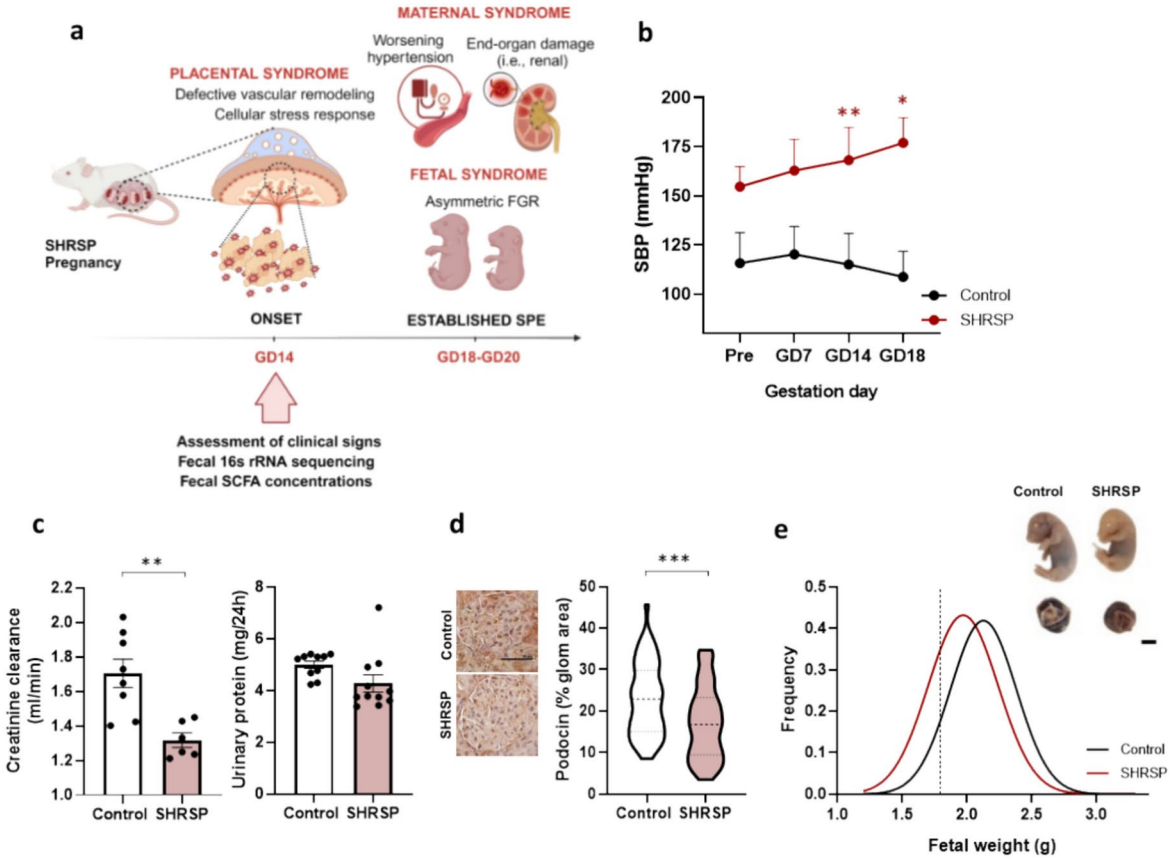

Fig. 1. Characterization of the SPE phenotype in the SHRSP model. (**a**) Model description and summary of experimental design (**b**) Maternal systolic blood pressure (SBP) profile. Data are mean ± SD of 8–10 animals/GD analyzed. Abbreviations: Pre, pre-mating (baseline) (**c**) Biochemical evaluation of renal function parameters on GD20, including creatinine clearance (left) and 24-h urinary protein content (right). Data shown are mean ± SEM derived from 6–11 rats per group each analyzed in duplicate. (**d**) Immunohistochemical assessment of podocin expression. Scale bar: 50 µm. Data are medians (dashed line) and minimum–maximum, n = 5–6 samples/group analyzing 40–100 glomeruli using QuPath. (**e**) Fetal weight frequency distribution, analyzed on GD20. The diagram shows the best-fit Gaussian curve for each group, resulting from the analysis of 82–88 fetal specimens corresponding to 8–6 litters per group. Dashed line: 10th percentile for the control group. Inset shows representative images of fetal and placental specimens for each group (scale: 5 mm). $^{*}p < 0.05$, $^{**}p < 0.01$, $^{***}p < 0.001$ as determined by two-way ANOVA and Tukey post hoc test (**b**) or Mann–Whitney *U* test (**c**,**d**).

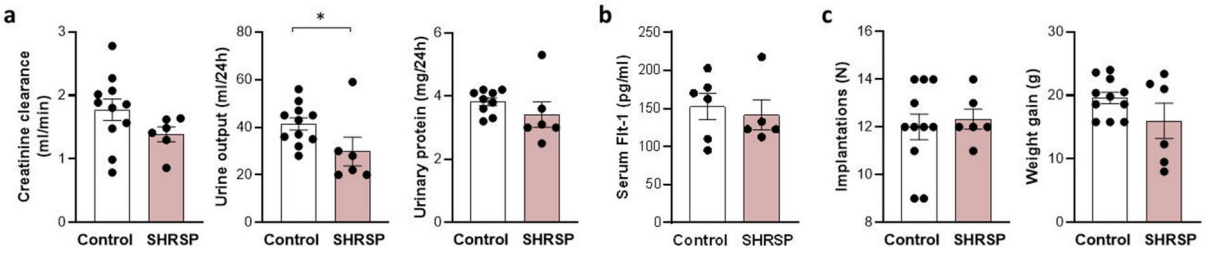

Fig. 2. Analysis of the SPE phenotype in control and SHRSP dams on GD14. (**a**) Assessment of biochemical markers of renal function including creatinine clearance, urine output and urinary protein content measured over a 24-h period. (**b**) Serum Flt-1 concentrations, as determined by ELISA. (**c**) Number of implantations per mother and maternal weight gain. Data shown are mean values ± SEM derived from 6–11 rats per group each analyzed in duplicate. $^{*}p < 0.05$, $^{**}p < 0.01$ as assessed by Student's *t*-test or Mann–Whitney *U* test.

higher relative abundance of *Prevotella* (SHRSP 0.32 ± 0.03 vs. Control 0.08 ± 0.01, $p < 0.001$) and lower relative abundance of *UCG-005* (an unclassified genus of *Oscillospiraceae,* SHRSP 0.011 ± 0.003 vs. Control 0.17 ± 0.03, $p < 0.01$) (Fig. 3a), as well as a lower *Firmicutes:Bacteroidetes* ratio (Fig. 3b). Alpha diversity (Shannon index) in the feces of SHRSP dams was lower on GD14 than in control animals (Fig. 2c), and principal component analysis (Beta diversity, Bray–Curtis dissimilarity index) revealed that the fecal microbiome of SHRSP had a large shift in the gut microbial community composition (Fig. 3d). These results show that at disease onset on GD14, SHRSP dams show a distinct profile of the gut microbiome, which displays a lower *Firmicutes*: *Bacteroidetes* ratio and is less diverse compared to controls.

Increased fecal SCFA concentrations at disease onset in the SHRSP correlate mildly with maternal signs

To characterize the microbial signature associated with disease onset at the functional level, we next assessed SCFA concentrations in the feces of control and SHRSP dams on GD14. As shown in Fig. 4a, acetate, propionate and valerate were significantly increased in SHRSP pregnancies compared to controls. Since there are known associations between PE, hypertension and gut bacterial metabolites, we next performed a correlation analysis to determine if these alterations in SCFA metabolism were associated with any of the clinical parameters measured in pregnant rats on GD14. Figure 4b demonstrates mild to moderate significant correlations of particular SCFAs with clinical parameters. We observed a positive correlation of valerate levels with systolic blood pressure ($rs = 0.472$, $p < 0.05$). Additionally, propionate ($rs = -0.472$, $p < 0.05$), butyrate ($rs = -0.557$, $p < 0.01$) and valerate ($rs = -0.424$, $p < 0.05$) all showed a significant negative correlation with urinary protein content, whereas propionate also correlated negatively with urine output ($rs = -0.539$, $p < 0.01$).

Correlation of specific enriched and depleted taxa in the SHRSP model with maternal signs and fecal SCFA concentrations

In order to identify the specific microbial signature of the SHRSP gut in the preclinical stage and understand its association with the development of maternal SPE signs, we next examined bacterial clades that were significantly enriched or depleted in SHRSP when compared with controls. We found that the relative abundance of *Prevotella*, *Bifidobacterium*, unclassified genera of *Prevotellaceae* and *Firmicutes* as well as *Parasutterella* and *Roseburia* were significantly increased in SHRSP feces on GD14, shown in Fig. 5a. Regarding depleted clades in these animals,

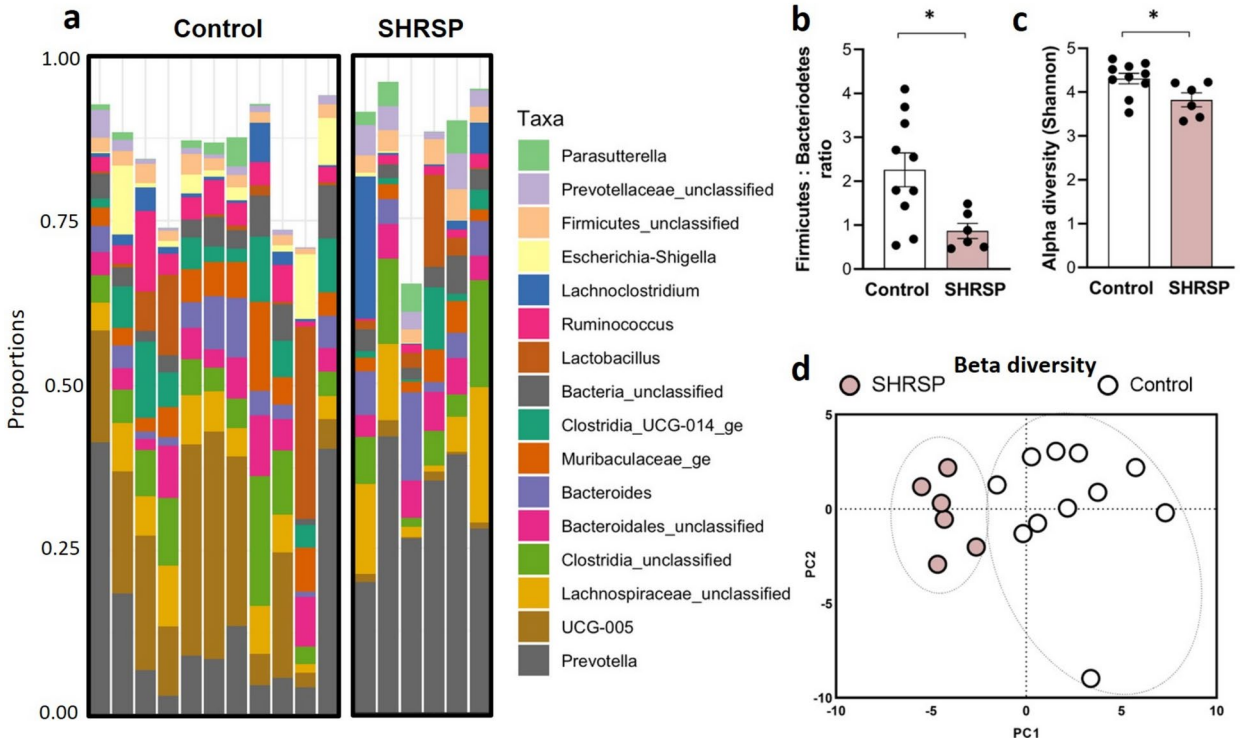

Fig. 3. Assessment of the GD14 fecal gut microbiota in control and SHRSP dams. (**a**) Taxonomic bar plots showing the relative abundance of 16S rRNA amplicon frequencies in the feces. White space on top of a bar represents lower-abundance taxa. Each bar represents one rat. (**b**) *Firmicutes:Bacteriodetes* ratio. (**c**) Alpha-diversity (Shannon Index). (**d**) Principal component analysis representing the beta diversity of the fecal bacterial communities. Data shown are mean values ± SEM derived from six to eleven rats per group each analyzed in duplicate. $^*p < 0.05$ as assessed by Student's *t*-test or Mann–Whitney *U* test of control versus SHRSP animals.

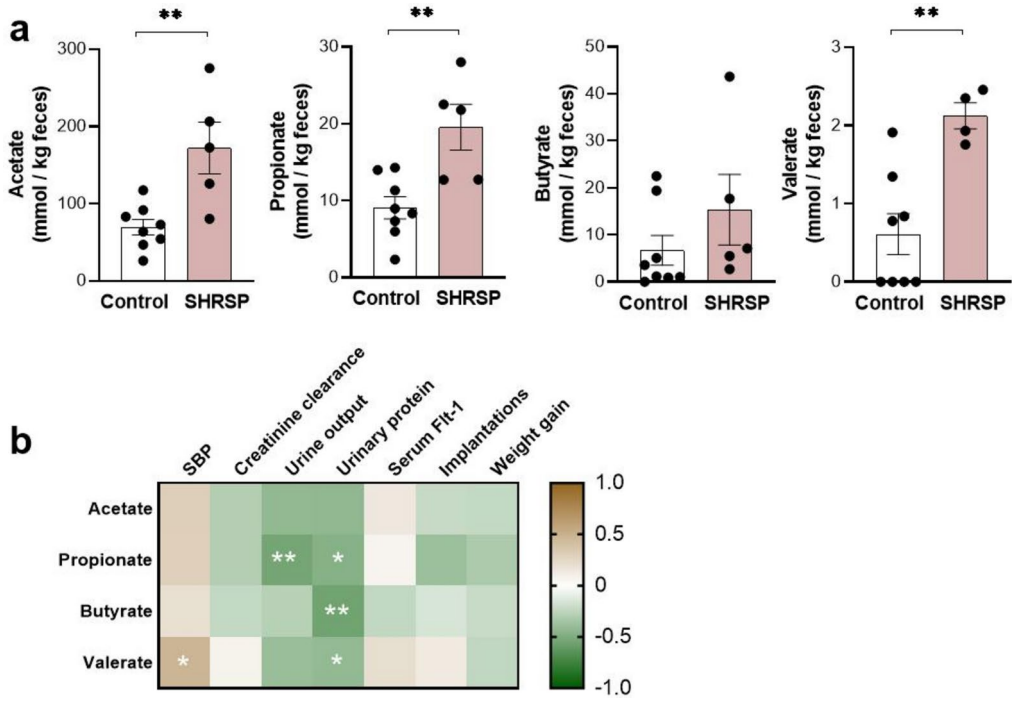

Fig. 4. Analysis of fecal SCFA concentrations in control and SHRSP pregnancies. (**a**) Concentrations of acetate, propionate, butyrate and valerate. Assessed by Student's *t*-test or Mann–Whitney *U* test. (**b**) Correlation heatmap reporting the comparison of SCFA concentrations with clinical parameters. The bar on the right shows the Spearman correlation coefficients. Significant *p* values for pairs of samples in the matrix are shown using white asterisks. Assessed by Spearman's rank correlation. Data shown are mean values ± SEM derived from five to eight rats per group each analyzed in duplicate. $^{*}p < 0.05$, $^{**}p < 0.01$.

we observed significantly lower relative abundance of *CAG-352* (*Ruminococcaceae*), *UCG-005* (an unclassified genus of *Oscillospiraceae*), *Blautia, Faecalibacterium* and *Ruminococcus*, shown in Fig. 5b.

We next performed Spearman R correlation analyses to determine the association between the enriched and depleted taxa with maternal signs and fecal SCFA levels. Figure 5c shows the correlation coefficients (Spearman rs) between specific taxa and maternal signs. The relative abundance of *Prevotella* (rs = 0.492, $p < 0.01$) and *Bifidobacterium* (rs = 0.682, $p < 0.001$) showed a strong positive correlation with systolic blood pressure. These enriched genera, along with unclassified *Prevotellaceae* correlated negatively with the kidney function parameters creatinine clearance and urine output. The stronger negative associations were observed between *Prevotella* and urine output (rs = −0.504, $p < 0.01$) and unclassified *Prevotellaceae* with creatinine clearance (rs = −0.611, $p < 0.001$). On the other hand, several of the genera that were depleted in SHRSP correlated negatively with systolic blood pressure and positively with kidney function parameters in pregnant rats. For example, the relative abundance of genus UCG-005 (rs = −0.827, $p < 0.001$), unclassified *Oscillospiraceae* (rs = −0.768, $p < 0.001$), and the genera *Blautia* (rs = −0.619, $p < 0.001$) and *Faecalibacterium* (rs = −0.609, $p < 0.001$) showed a strong negative correlation with systolic blood pressure. A strong positive correlation was observed between the relative abundance of *CAG-352* and urine output (rs = 0.689, $p < 0.001$) and also *Faecalibacterium* and creatinine clearance (rs = 0.583, $p < 0.001$). Of note, several of the genera depleted in SHRSP including *CAG-352*, the unclassified *Oscillospiraceae*, UCG-005, *Blautia* and *Faecalibacterium* showed a mild positive correlation with maternal weight gain.

As for fecal SCFA levels, we observed a strong positive correlation between bacterial genera enriched in the SHRSP gut and concentrations of acetate, propionate and valerate (Fig. 5d). For instance, acetate and propionate levels correlated significantly with the relative abundance of *Prevotella* ($rs_{acetate} = 0.582$, $rs_{propionate} = 0.571$, $p < 0.01$), unclassified *Prevotellaceae* ($rs_{acetate} = 0.546$, $rs_{propionate} = 0.609$, $p < 0.01$) and *Bifidobacterium* ($rs_{acetate} = 0.480$, $rs_{propionate} = 0.499$, $p < 0.05$). Interestingly, the stronger positive correlations were found between fecal valerate concentrations and the top-enriched taxa *Prevotella* (rs = 0.574, $p < 0.01$), *Bifidobacterium* (rs = 0.664, $p < 0.01$) along with unclassified genera of *Prevotellaceae* (rs = 0.586, $p < 0.01$) and *Firmicutes* (rs = 0.624, $p < 0.01$). In contrast, most genera that were depleted in the SHRSP gut compared to controls showed a negative correlation with fecal concentrations of acetate, propionate and valerate. The stronger associations were between *CAG-352* and acetate (rs = −0.571, $p < 0.01$), propionate (rs = −0.718, $p < 0.001$) and valerate (rs = −0.593, $p < 0.01$); and between Ruminococcus and valerate (rs = −0.592, $p < 0.01$).

Discussion

In this study, we show that the SHRSP model displays a distinct gut microbial signature along with altered SCFA metabolism compared to control pregnancies on GD14, a time point that marks the pre-clinical stage of SPE

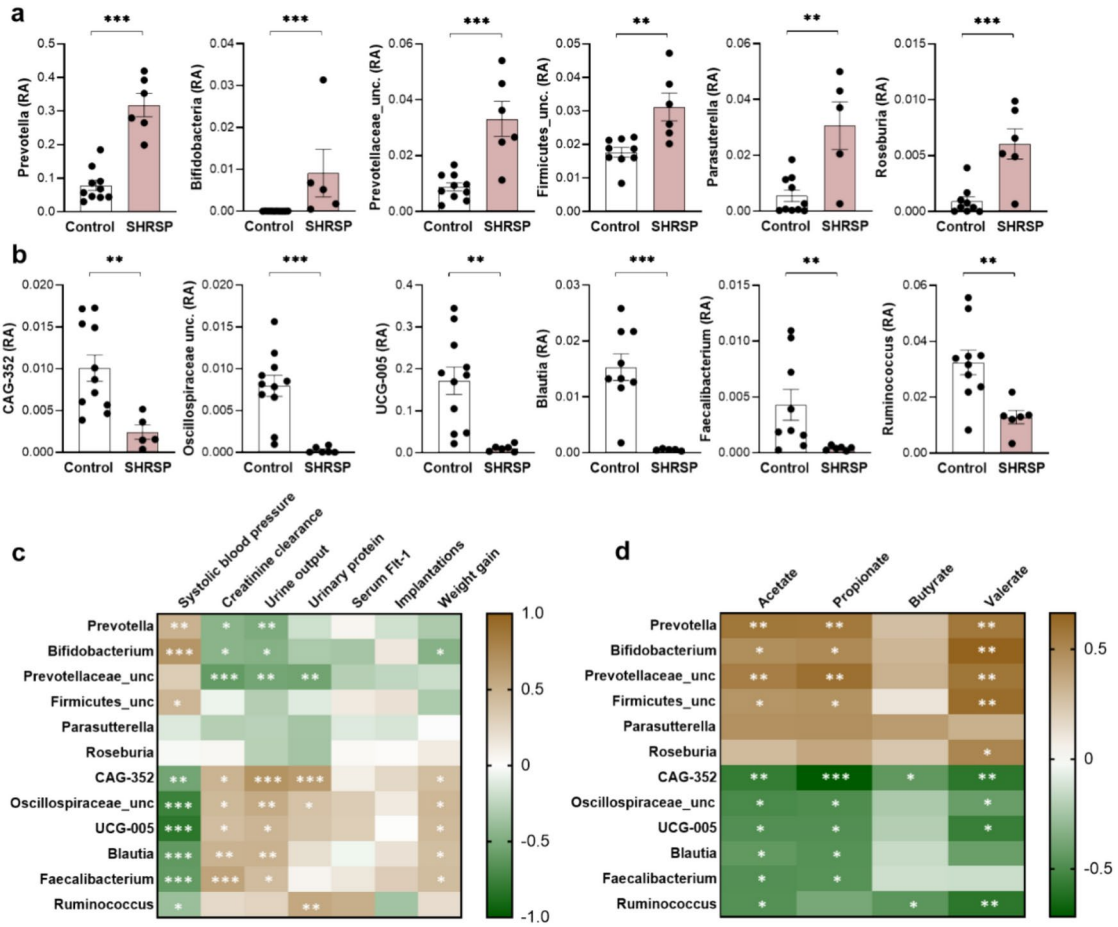

Fig. 5. Analysis of the top twelve enriched and depleted genera measured in feces from GD14 control and SHRSP dams. (**a**) Relative abundance of the top six enriched genera: *Prevotella*, *Bifidobacterium*, *Prevotellaceae*-unclassified, *Firmicutes*, *Parasutterella* and *Roseburia.* (**b**) Relative abundance of the top 6 depleted genera: *CAG-352* (family *Ruminococcaceae*), *Oscillospiraceae*-unclassified, *UCG-005* (family *Oscillospiraceae*), *Blautia, Faecalibacterium* and *Ruminococcus.* (**c**) Correlation heatmap comparing bacterial relative abundance with clinical parameters. The bar on the right shows the Spearman correlation coefficients. Significant *p* values for pairs of samples in the matrix are shown using white asterisks. (**d**) Spearman correlation analysis of bacterial relative abundance with fecal SCFA concentrations. *RA* relative abundance, *Unc* unclassified. Data shown are mean values ± SEM derived from six to eleven rats per group each analyzed in duplicate. $^{*}p < 0.05$ $^{**}p < 0.01$, $^{***}p < 0.001$. (**a**,**b**) Assessed by Student's *t*-test or Mann–Whitney *U* test. (**c**,**d**) Assessed by Spearman's rank correlation.

progression and is known to be coincident with defective placentation processes[4,6]. Our analyses revealed that disease onset in this model (characterized by mild alterations in renal function), was associated with marked differences in the gut bacterial community that correlate strongly with the future clinical manifestations of the syndrome. The GD14 fecal microbiome from the SHRSP group had a lower alpha diversity and decreased *Firmicutes:Bacteriodetes* ratio compared to the control group. At the genus level, SHRSP dams showed a distinct profile with enrichment of *Prevotella*, *Bifidobacterium*, *Parasutterella* and *Roseburia* compared to controls, showing a strong correlation with clinical parameters and fecal SCFA concentrations. On the other hand, genera *CAG-352* (family *Ruminococcaceae*), *UCG-005* (family *Oscillospiraceae*), *Blautia* and *Faecalibacterium* that were abundant in control pregnancies, were found to be largely depleted from the SHRSP microbiome at onset of disease.

Cumulative evidence supports a role for gut microbial dysbiosis in the pathogenesis of hypertension[8,20–22] and hypertensive disorders of pregnancy including PE[10,23–25]. In PE patients specifically, gut dysbiosis is characterized by decreased alpha diversity, and at the phylum level, depletion of *Firmicutes* and increased abundance of *Proteobacteria*, *Bacteroidota* and *Actinobacteria*[25,26]. These differences were largely mirrored by the lower diversity and the top enriched and depleted genera we observed in pregnant SHRSP compared to control animals, further validating this strain as a preclinical model that reproduces pathogenic traits present in preeclamptic pregnancies. As we have characterized the SHRSP gut microbial signature at the pre-clinical stage before the establishment of major maternal signs, our finding may have important implications for the assessment of high-risk human pregnancies with preexisting hypertension.

Among the top enriched bacteria, the SHRSP gut environment appeared to be dominated by the genus *Prevotella.* A *Prevotella*-dominated enterotype has been described in patients with hypertension[8], and intestinal expansion of this genus has also been associated with the inflammatory response driving the pathogenesis of rheumatoid arthritis[27]. More recently, enrichment of *Prevotella* in the vaginal microbiome was reported associated with elevated systemic TNFa levels in patients with severe PE[28]. Species of *Prevotella* (i.e., *P. intermedia, P. nigrescens*) are also involved in the pathogenesis of periodontal disease, which is a well-documented risk factor for adverse pregnancy outcomes including PE[29–31]. The mechanism underlying this association involves an exaggerated placental and systemic inflammatory response caused by the hematogenous spread of periodontal pathogens and their byproducts[32,33]. Since Spontaneously Hypertensive Rats (SHR, the parental strain for the SHRSP model) are known to have barrier dysfunction due to decreased expression of intestinal tight junction proteins[34], and recent studies suggest a role for intestinal leakage and bacterial translocation in promoting PE in pregnant mice[35], our findings argue that bacterial components derived from the dysbiotic maternal gut may contribute to SPE pathogenesis in the SHRSP model. As for the depleted OTUs in SHRSP pregnancies, the most representative were genera of the phylum Firmicutes (*UCG-005*, *Blautia* and *Ruminococcus*) well-known for their capacity to produce anti-inflammatory SCFAs, which have been reported as protective bacteria in hypertension[8,20,36] and PE[10,25,26]. Interestingly, the bacteria that were depleted in SHRSP pregnancies appeared to have a stronger correlation with clinical parameters than enriched genera. This indicates that enrichment of particular bacterial species in the gut or supplementation of specific metabolites produced by these taxa may represent a promising approach for prevention in women at risk for SPE.

Conflicting results exist regarding particular OTU that were reported as enriched or depleted in our model when compared with previous studies in human subjects. For instance, depletion of *Prevotella* was reported in the gut microbiome of early-onset PE at antepartum[10], and reduced abundance of genus *Bifidobacterium* was reported by two independent studies comparing the gut microbial signature of healthy pregnancy vs. PE patients[37] or severe PE patients[25] during the third trimester. Moreover, although Chang et al[25] reported depletion of *Blautia* in PE like in the present study, the study by Miao et al. found an increased abundance of this genus as well as *Ruminococcus* in PE[37]. Several studies have reported a depletion of *Akkermansia* in PE subjects suggesting a protective effect of this genus[10,35,38,39], but we found no evidence of its involvement in the microbial signature associated with the onset of disease in our model. These discrepancies may be explained on the one hand by differences in gestational age as unlike our study, the majority of human studies have been conducted during the third trimester when the maternal syndrome is fully established. On the other hand, they may reflect the heterogeneity of the PE syndrome in terms of molecular pathways, symptoms, and clinical outcomes[40], which is one of the main limitations for early and accurate diagnosis. Indeed, it is plausible that rather than being promoted by a particular core set of OTUs associated with disease, there is some degree of functional redundancy in the microbiome driving PE progression.

An interesting finding in our study was the higher fecal SCFA concentrations observed on GD14 in SHRSP pregnancies compared to control animals, which may be a direct consequence of increased production by the microbial taxa enriched in the maternal gut. For instance, *Prevotella* and *Parasutterella* are known for their ability to metabolize dietary fiber and produce acetate[41] and succinate[41,42], which is a precursor for propionate biosynthesis. Increased fecal SCFA levels have been reported in human studies of hypertension[36,43,44] and also in animal models[45,46], often showing an opposite trend with SCFA measurements in circulation. Efficient colonic absorption of SCFA results in less than 5% being excreted in the feces, and it has been suggested that fecal measurements are more representative of intestinal SCFA uptake than production[47]. Thus, the higher fecal SCFA levels observed in SHRSP likely reflect poor intestinal absorption related to the hypertensive condition, as supported by previous studies demonstrating a marked decrease in the colonic expression of the SCFA transporters *Scl5a8*/SMCT1, MCT1 and MCT4[46,48,49] in the SHR gut. Indeed, observations in prehypertensive SHR and angiotensin II infused rats suggest that pathological changes in the gut including increased permeability, altered tight junction expression and inflammation associated with enhanced sympathetic input to the gut wall play an important role in the development of hypertension[34]. In this context, inefficient intestinal absorption of SCFA in the SHRSP model may account for the finding that, unlike specific bacterial taxa, SCFA concentrations showed a weak correlation with the clinical parameters assessed in our study.

Blood pressure regulation by SCFAs results from the engagement of G-protein-coupled receptors present in the vasculature[50], with GPR41 and GPR43 being responsible for the vasorelaxant effect of the major SCFAs acetate, propionate and butyrate. Reduced expression of these receptors is associated with arterial stiffness, and has been reported in mesenteric resistance arteries in SHR[49], suggesting that impaired vascular SCFA signaling may contribute to hypertension in this model. Notably, of the SCFAs analyzed in our study valerate showed the stronger correlation with enriched microbial taxa and a mild but significant positive correlation with SBP measurements. Little is currently known about the biology of this SCFA and while its fecal concentrations were low in this study, it has been reported that rapid valerate absorption in the colon results in serum levels comparable to propionate and butyrate[51,52]. Interestingly, valerate has been shown to reprogram lymphocyte metabolism in vivo and induce IL10 production by $CD4^+$ T and B regulatory cells[53], which may be relevant to the maintenance of fetomaternal tolerance during pregnancy. Considering these evidences, together with studies showing a marked reduction in fecal valerate levels in PE patients[25] and animal studies demonstrating a significant decrease of blood pressure via GPR41/43 signaling upon colonic infusion of sodium valerate[52], research on the role of this particular SCFA in hypertensive disorders of pregnancy should be encouraged.

Given the weak correlation of SCFA levels with clinical SPE signs, it is also possible that other bacterial metabolites from the dysbiotic SHRSP gut promote SPE in this model. For instance, *Prevotellaceae* are also known to produce trimethylamine (TMA)[54], which in its N-oxidized form (TMAO) shows a pro-atherogenic effect that is considered an important risk factor for cardiovascular disease[55]. Elevated circulating TMAO has been reported in PE patients, showing a positive correlation with markers of systemic inflammation and

endothelial dysfunction[26,56]. Interestingly, increased TMAO was recently reported to mediate hypertension and endothelial dysfunction in RUPP rats[57], in which PE signs develop as a result of surgical induction of placental ischemia. Considering reports in the SHR showing an increased gut permeability to TMA[58], involvement of this metabolite in the development of SPE and its association with impaired spiral artery remodeling as observed in the SHRSP model[4] merits further investigation.

The maternal gut microbiome undergoes substantial changes during a normal pregnancy, showing a progressive reduction in alpha diversity towards term and enrichment in *Proteobacteria*, *Actinobacteria* and lactate producers so that the profile becomes more resemblant of the dysbiosis associated with obesity and cardiometabolic disease[17]. This pregnancy-specific remodeling of the gut microbiome occurs in a physiological context and appears to contribute to the hormonal, metabolic and immune adaptations required for normal placental development and fetal growth. A limitation of the present study is that we did not assess the SHRSP microbiome in the non-pregnant status, which limits our ability to discern the microbial alterations related to the pre-existing hypertension from those specific of the pregnant status. Nevertheless, our findings at disease onset in the SHRSP together with observations on the Dahl S rat (another model of pre-existing hypertension with SPE[59]) suggest that the gut dysbiosis associated with the hypertensive status may interfere with the physiological remodeling of the maternal microbiome necessary for a healthy gestation. Furthermore, since Bacteroidetes are a major contributor to the LPS biosynthesis pathway, another potential mechanism by which the dysbiotic profile associated with chronic hypertension may favor the development of PE is through increasing the systemic inflammatory burden in the non-pregnant status. This would create a high-risk niche sensitive to further perturbations resulting from aberrant immune interactions during placental development, ultimately amplifying the inflammatory cascade leading to endothelial dysfunction and maternal manifestations of the disease.

In summary, our study characterized the gut microbial signature associated with PE onset in the SHRSP model, showing an enrichment in *Prevotella*, *Bifidobacterium*, *Parasutterella* and *Roseburia* and increased fecal concentrations of the SCFA acetate, propionate and valerate. Since these alterations were present in the preclinical stage of the syndrome and showed a strong correlation with maternal signs, we speculate that further assessment of the microbial signature and its associated metabolites could potentially contribute to improve PE diagnosis. Furthermore, the SHRSP and other spontaneous preclinical models of PE represent useful tools to study the impact of the microbiome at each stage of pregnancy with regard to placental function and offspring health outcomes, contributing to a better understanding of the so-called gut-placenta axis. Recent studies have demonstrated the involvement of gut microbial signals in the modulation of several processes related to placental development and function including trophoblast invasion[38,60], spiral artery remodeling[38], branching morphogenesis and nutrient transporter expression[61]. In this context, since the distinct gut microbial signature identified in this study coincides with major defects in trophoblast differentiation, spiral artery remodeling and activation of placental oxidative stress pathways that we previously reported in SHRSP pregnancies[4,5], we anticipate that in an depth characterization of the gut-placenta axis in this model, including assessment of other bacterial metabolites as well as their receptors, will provide important clues on the role of microbiome-derived signals in driving placental development and promoting PE in high-risk pregnancies.

Methods

Ethical approval

All experiments were conducted according to the National Institutes of Health Guide for the Care and Use of Laboratory Animals and reported in compliance with ARRIVE guidelines. The study was approved by the Institutional Animal Care Committee (CICUAL, Facultad de Medicina, Universidad de Buenos Aires).

Experimental design and disease model

Female SHRSP (SPE—model) and Wistar Kyoto (WKY—Control) rats that were 10–12 weeks old, weighing 200–250 g, were mated to congenic males and checked daily for vaginal plugs, denoted as gestation day GD1. During the experiment, pregnant females of each strain were co-housed in groups of up to 4 rats per cage with access to food and water ad libitum. On GD14, dams were placed individually in clean empty cages for collection of freshly excreted fecal samples, which were flash frozen in liquid nitrogen and stored at − 80 °C until further analysis.

Determination of the SPE phenotype

Blood pressure determination

Systolic blood pressure (SBP) profiles were determined in conscious rats restrained in a thermal plastic chamber using a tail-cuff device (CODA 2—Kent Scientific), as described previously[6]. Measurements were performed in the morning with an acclimation of five cuff inflations, followed by 20 measurement cycles. Values were averaged and rare outliers (± 2 SD from the mean) were eliminated. SBP was expressed as the mean from at least 10 remaining values.

Biochemical determinations in serum and urine samples

Pregnant females were housed individually in metabolic cages on the morning of GD13 or GD19 and urine samples were collected over a 24-h period with food and water provided ad libitum. After recording urinary output and maternal body weight, urine samples were stored at − 20 °C for future analysis. Blood samples were collected from the abdominal aorta under anesthesia (thiopental sodium 40 mg/kg body weight, i.p.) prior to euthanasia by intracardiac anesthetic overdose for tissue collection. Urine and serum samples were assayed for creatinine content using the enzymatic ultraviolet method (Randox Laboratories), and urinary protein (24 h proteinuria) was determined by a standard turbidimetric assay. Creatinine clearance was calculated according

to the standard formula as described previously[4]. Serum samples were assayed for Flt-1 concentrations using a commercial ELISA kit (#MVR100, R&D Systems).

Histological assessment of renal damage

Kidney damage was determined by evaluating the expression of the podocyte marker podocin following a standard immunoperoxidase protocol, as described previously[6]. Briefly, 4-µm sections were deparaffinized, rehydrated and incubated for 30 min in 3% H_2O_2 in PBS for quenching of endogenous peroxidase activity. The sections were then washed in PBS (pH 7.2) for 20 min, followed by incubation with blocking serum for 20 min. The primary antibody (podocin, sc-21009, Santa Cruz Biotechnology; 1:200) was incubated for 1 h at room temperature. Following incubation with a biotinylated universal antibody (SS Multilink, Biogenex) for 30 min, the signal was detected using a liquid diaminobenzidine (DAB) Substrate Chromogen System (cat. #K3467, DAKO). After washing, nuclei were counterstained with 0.1% Mayer's hematoxylin, followed by a standard dehydration procedure and mounting in a DPX histology medium (Millipore-Sigma). Photo documentation was performed using a Nikon E400 microscope and podocin expression was determined as the DAB-positive glomerular area fraction using the thresholder algorithm of QuPath v0.4.4 software[62].

Assessment of fetal phenotype

Fetoplacental specimens were collected from euthanized GD14 rats, and the number of viable and resorbed implantation sites was recorded. GD14 specimens were stored phosphate-buffered 10% formaldehyde (pH 7.2) for further analyses.

The FGR phenotype was assessed morphometrically on GD20. Briefly, following collection of amniotic fluid, the amnion was dissected to expose the fetuses and placentas, which were fixed in phosphate-buffered 10% formaldehyde (pH 7.2). Fetal weight was recorded from the fixed specimens as described previously[6].

Molecular analysis of the fecal microbiome and SCFAs

16S rRNA sequencing

Gut microbiome profiles from GD14 rat feces were assessed by MiSeq 16S rRNA sequencing of V4 amplicons using the following procedure. Pooled DNA samples were sent to Microbiome Insights (Vancouver, Canada) for sequencing and analysis. The 16S ribosomal RNA genes (V4 region) was sequenced on an Illumina MiSeq (v. 2 chemistry) using the dual barcoding protocol of Kozich et al.[63]. Primers and PCR conditions used for 16S sequencing are identical to those of Kozich et al.[63]. Bacterial Raw Fastq files were quality-filtered and clustered into 97% similarity operational taxonomic units (OTUs) using the mothur software package (v. 1.44.1)[64], following the recommended procedure (https://www.mothur.org/wiki/MiSeq_SOP; accessed March 2021). Paired-end reads were merged and curated to reduce sequencing error[65]. Chimeric sequences were identified and removed using UCHIME[66]. The curated sequences were assigned to OTUs at 97% similarity using the OptiClust algorithm[67] and classified to the deepest taxonomic level that had 80% support using the naive Bayesian classifier trained on the Silva data base (v132).

SCFA analysis

Fecal SCFA content was analyzed using gas chromatography (HP 5890 series II—Hewlett Packard) coupled to a flame ionization detector. After dilution and centrifugation of the feces, the supernatant was mixed with 1 M NaOH, 0.36 M HClO4 and 2-ethylbutyric acid as an internal standard. After overnight lyophilization, the pellet was redissolved in 5 M formic acid and 400 µl acetone, centrifuged and 1 ml of the supernatant was injected into the gas chromatograph.

Microbiome biostatistical analyses

Alpha diversity was calculated using Shannon's diversity index on raw count ASV table after filtering out contaminants using the Phyloseq R package[68]. The significance of diversity differences was tested with one-way ANOVA with Tukey's post hoc test (diversity value ~ Group). OTU abundances were summarized with the Bray–Curtis index and a principal coordinate analysis (PCoA) was performed to visualize microbiome similarities. Variation in microbial diversity was assessed with permutational multivariate analyses of variance (adonis in R) with group as factors using 9999 permutations for significance testing. Differential abundance testing was performed using Deseq2 method[69]. Significant taxa was determined by the adjusted p-value (FDR < 0.05) and the absolute log2 fold change (value > 2). All analyses were conducted in the R environment (R-Core-Team, 2019). Data were plotted using the ggplot2 R package[70].

Statistical analysis

The normal distribution of samples was assessed using a Shapiro–Wilk normality test. Student's *t*-test or Mann Whitney *U* tests were used to analyze normal and skewed data respectively. Correlation analysis was performed using Spearman's rank correlation. Graphing and statistical tests were performed using the software GraphPad Prism 9.

Data availability

The data that support the findings of this study are available from the corresponding author upon reasonable request. Sequencing data are deposited under BioProject accession number PRJNA1176534 (http://www.ncbi.nlm.nih.gov/bioproject/1176534).

Received: 11 September 2023; Accepted: 18 December 2024

Published online: 30 December 2024

References

1. Kametas, N. A., Nzelu, D. & Nicolaides, K. H. Chronic hypertension and superimposed preeclampsia: screening and diagnosis. *Am. J. Obstet. Gynecol.* **226**, S1182–S1195. https://doi.org/10.1016/j.ajog.2020.11.029 (2022).
2. Rezk, M., Gamal, A. & Emara, M. Maternal and fetal outcome in de novo preeclampsia in comparison to superimposed preeclampsia: a two-year observational study. *Hypertens. Pregnancy* **34**, 137–144. https://doi.org/10.3109/10641955.2014.982329 (2015).
3. Valent, A. M. et al. Expectant management of mild preeclampsia versus superimposed preeclampsia up to 37 weeks. *Am. J. Obstet. Gynecol.* **212**(515), e511-518. https://doi.org/10.1016/j.ajog.2014.10.1090 (2015).
4. Barrientos, G. et al. Defective trophoblast invasion underlies fetal growth restriction and preeclampsia-like symptoms in the stroke-prone spontaneously hypertensive rat. *Mol. Hum. Reprod.* **23**, 509–519. https://doi.org/10.1093/molehr/gax024 (2017).
5. Blois, S. M., Prince, P. D., Borowski, S., Galleano, M. & Barrientos, G. Placental glycoredox dysregulation associated with disease progression in an animal model of superimposed preeclampsia. *Cells* **10**. https://doi.org/10.3390/cells10040800 (2021).
6. Barrientos, G. et al. Therapeutic effect of alpha lipoic acid in a rat preclinical model of preeclampsia: focus on maternal signs, fetal growth and placental function. *Antioxidants* **13**, 730 (2024).
7. Stiemsma, L. T. & Michels, K. B. The role of the microbiome in the developmental origins of health and disease. *Pediatrics* **141**. https://doi.org/10.1542/peds.2017-2437 (2018).
8. Li, J. et al. Gut microbiota dysbiosis contributes to the development of hypertension. *Microbiome* **5**, 14. https://doi.org/10.1186/s40168-016-0222-x (2017).
9. Yang, T. et al. Gut dysbiosis is linked to hypertension. *Hypertension* **65**, 1331–1340. https://doi.org/10.1161/HYPERTENSIONAHA.115.05315 (2015).
10. Lv, L. J. et al. Early-onset preeclampsia is associated with gut microbial alterations in antepartum and postpartum women. *Front. Cell Infect. Microbiol.* **9**, 224. https://doi.org/10.3389/fcimb.2019.00224 (2019).
11. Ley, R. E., Turnbaugh, P. J., Klein, S. & Gordon, J. I. Microbial ecology: human gut microbes associated with obesity. *Nature* **444**, 1022–1023. https://doi.org/10.1038/4441022a (2006).
12. Kaye, D. M. et al. Deficiency of prebiotic fiber and insufficient signaling through gut metabolite-sensing receptors leads to cardiovascular disease. *Circulation* **141**, 1393–1403. https://doi.org/10.1161/CIRCULATIONAHA.119.043081 (2020).
13. Chakraborty, S. et al. Metabolites and Hypertension: Insights into Hypertension as a Metabolic Disorder: 2019 Harriet Dustan Award.
14. Shi, H. et al. Alterations of the gut microbial community structure and function with aging in the spontaneously hypertensive stroke prone rat. *Sci. Rep.* **12**, 8534. https://doi.org/10.1038/s41598-022-12578-7 (2022).
15. Adnan, S. et al. Alterations in the gut microbiota can elicit hypertension in rats. *Physiol. Genomics* **49**, 96–104. https://doi.org/10.1152/physiolgenomics.00081.2016 (2017).
16. Nelson, J. W. et al. The gut microbiome contributes to blood-brain barrier disruption in spontaneously hypertensive stroke prone rats. *FASEB J.* **35**, e21201. https://doi.org/10.1096/fj.202001117R (2021).
17. Koren, O. et al. Host remodeling of the gut microbiome and metabolic changes during pregnancy. *Cell* **150**, 470–480. https://doi.org/10.1016/j.cell.2012.07.008 (2012).
18. Siena, M. et al. Gut and reproductive tract microbiota adaptation during pregnancy: new insights for pregnancy-related complications and therapy. *Microorganisms* **9**. https://doi.org/10.3390/microorganisms9030473 (2021).
19. Small, H. Y. et al. Abnormal uterine artery remodelling in the stroke prone spontaneously hypertensive rat. *Placenta* **37**, 34–44. https://doi.org/10.1016/j.placenta.2015.10.022 (2016).
20. Yan, Q. et al. Alterations of the gut microbiome in hypertension. *Front. Cell Infect. Microbiol.* **7**, 381. https://doi.org/10.3389/fcimb.2017.00381 (2017).
21. Kim, S. et al. Imbalance of gut microbiome and intestinal epithelial barrier dysfunction in patients with high blood pressure. *Clin. Sci. (Lond)* **132**, 701–718. https://doi.org/10.1042/CS20180087 (2018).
22. Karbach, S. H. et al. Gut microbiota promote angiotensin II-induced arterial hypertension and vascular dysfunction. *J. Am. Heart Assoc.* **5**. https://doi.org/10.1161/JAHA.116.003698 (2016).
23. Lin, H. et al. The association between gut microbiome and pregnancy-induced hypertension: a nested case-control study. *Nutrients* **14**. https://doi.org/10.3390/nu14214582 (2022).
24. Wu, J., Zhang, D., Zhao, M. & Zheng, X. Gut microbiota dysbiosis and increased NLRP3 levels in patients with pregnancy-induced hypertension. *Curr. Microbiol.* **80**, 168. https://doi.org/10.1007/s00284-023-03252-w (2023).
25. Chang, Y. et al. Short-chain fatty acids accompanying changes in the gut microbiome contribute to the development of hypertension in patients with preeclampsia. *Clin. Sci. (Lond)* **134**, 289–302. https://doi.org/10.1042/CS20191253 (2020).
26. Wang, J., Gu, X., Yang, J., Wei, Y. & Zhao, Y. Gut Microbiota dysbiosis and increased plasma LPS and TMAO levels in patients with preeclampsia. *Front. Cell Infect. Microbiol.* **9**, 409. https://doi.org/10.3389/fcimb.2019.00409 (2019).
27. Scher, J. U. et al. Expansion of intestinal *Prevotella copri* correlates with enhanced susceptibility to arthritis. *Elife* **2**, e01202. https://doi.org/10.7554/eLife.01202 (2013).
28. Lin, C. Y. et al. Severe preeclampsia is associated with a higher relative abundance of *Prevotella bivia* in the vaginal microbiota. *Sci. Rep.* **10**, 18249. https://doi.org/10.1038/s41598-020-75534-3 (2020).
29. Cota, L. O., Guimaraes, A. N., Costa, J. E., Lorentz, T. C. & Costa, F. O. Association between maternal periodontitis and an increased risk of preeclampsia. *J. Periodontol.* **77**, 2063–2069. https://doi.org/10.1902/jop.2006.060061 (2006).
30. Le, Q. A. et al. Periodontitis and preeclampsia in pregnancy: a systematic review and meta-analysis. *Matern. Child Health J.* **26**, 2419–2443. https://doi.org/10.1007/s10995-022-03556-6 (2022).
31. Tanneeru, S., Mahendra, J. & Shaik, M. V. Evaluation of microflora (viral and bacterial) in subgingival and placental samples of pregnant women with preeclampsia with and without periodontal disease: a cross-sectional study. *J. Int. Soc. Prev. Community Dent.* **10**, 171–176. https://doi.org/10.4103/jispcd.JISPCD_341_19 (2020).
32. Ruma, M. et al. Maternal periodontal disease, systemic inflammation, and risk for preeclampsia. *Am. J. Obstet. Gynecol.* **198**(389), e381-385. https://doi.org/10.1016/j.ajog.2007.12.002 (2008).
33. Parthiban, P. S. et al. Association between specific periodontal pathogens, Toll-like receptor-4, and nuclear factor-kappaB expression in placental tissues of pre-eclamptic women with periodontitis. *J. Investig. Clin. Dent.* **9**. https://doi.org/10.1111/jicd.12265 (2018).
34. Santisteban, M. M. et al. Hypertension-linked pathophysiological alterations in the gut. *Circ. Res.* **120**, 312–323. https://doi.org/10.1161/CIRCRESAHA.116.309006 (2017).
35. Chen, X. et al. Gut dysbiosis induces the development of pre-eclampsia through bacterial translocation. *Gut* **69**, 513–522. https://doi.org/10.1136/gutjnl-2019-319101 (2020).
36. Calderon-Perez, L. et al. Gut metagenomic and short chain fatty acids signature in hypertension: a cross-sectional study. *Sci. Rep.* **10**, 6436. https://doi.org/10.1038/s41598-020-63475-w (2020).
37. Miao, T. et al. Decrease in abundance of bacteria of the genus Bifidobacterium in gut microbiota may be related to pre-eclampsia progression in women from East China. *Food Nutr. Res.* **65**. https://doi.org/10.29219/fnr.v65.5781 (2021).

38. Jin, J. et al. Gut dysbiosis promotes preeclampsia by regulating macrophages and trophoblasts. *Circ. Res.* **131**, 492–506. https://doi.org/10.1161/CIRCRESAHA.122.320771 (2022).
39. Meijer, S. et al. Gut micro- and mycobiota in preeclampsia: bacterial composition differences suggest role in pathophysiology. *Biomolecules* **13**. https://doi.org/10.3390/biom13020346 (2023).
40. Than, N. G. et al. Early pathways, biomarkers, and four distinct molecular subclasses of preeclampsia: The intersection of clinical, pathological, and high-dimensional biology studies. *Placenta* **125**, 10–19. https://doi.org/10.1016/j.placenta.2022.03.009 (2022).
41. Franke, T. & Deppenmeier, U. Physiology and central carbon metabolism of the gut bacterium *Prevotella copri*. *Mol. Microbiol.* **109**, 528–540. https://doi.org/10.1111/mmi.14058 (2018).
42. Ju, T., Kong, J. Y., Stothard, P. & Willing, B. P. Defining the role of Parasutterella, a previously uncharacterized member of the core gut microbiota. *ISME J.* **13**, 1520–1534. https://doi.org/10.1038/s41396-019-0364-5 (2019).
43. de la Cuesta-Zuluaga, J. et al. Higher fecal short-chain fatty acid levels are associated with gut microbiome dysbiosis, obesity, hypertension and cardiometabolic disease risk factors. *Nutrients* **11**. https://doi.org/10.3390/nu11010051 (2018).
44. Guo, Y., Li, X., Wang, Z. & Yu, B. Gut microbiota dysbiosis in human hypertension: a systematic review of observational studies. *Front. Cardiovasc. Med.* **8**, 650227. https://doi.org/10.3389/fcvm.2021.650227 (2021).
45. Bier, A. et al. A high salt diet modulates the gut microbiota and short chain fatty acids production in a salt-sensitive hypertension rat model. *Nutrients* **10**. https://doi.org/10.3390/nu10091154 (2018).
46. Yang, T. et al. Impaired butyrate absorption in the proximal colon, low serum butyrate and diminished central effects of butyrate on blood pressure in spontaneously hypertensive rats. *Acta Physiol. (Oxf)* **226**, e13256. https://doi.org/10.1111/apha.13256 (2019).
47. Vogt, J. A. & Wolever, T. M. Fecal acetate is inversely related to acetate absorption from the human rectum and distal colon. *J. Nutr.* **133**, 3145–3148. https://doi.org/10.1093/jn/133.10.3145 (2003).
48. Robles-Vera, I. et al. Probiotics prevent dysbiosis and the rise in blood pressure in genetic hypertension: role of short-chain fatty acids. *Mol. Nutr. Food Res.* **64**, e1900616. https://doi.org/10.1002/mnfr.201900616 (2020).
49. Dardi, P. et al. Reduced intestinal butyrate availability is associated with the vascular remodeling in resistance arteries of hypertensive rats. *Front. Physiol.* **13**, 998362. https://doi.org/10.3389/fphys.2022.998362 (2022).
50. Pluznick, J. L. Microbial short-chain fatty acids and blood pressure regulation. *Curr. Hypertens. Rep.* **19**, 25. https://doi.org/10.1007/s11906-017-0722-5 (2017).
51. Jakobsdottir, G., Bjerregaard, J. H., Skovbjerg, H. & Nyman, M. Fasting serum concentration of short-chain fatty acids in subjects with microscopic colitis and celiac disease: no difference compared with controls, but between genders. *Scand. J. Gastroenterol.* **48**, 696–701. https://doi.org/10.3109/00365521.2013.786128 (2013).
52. Onyszkiewicz, M. et al. Valeric acid lowers arterial blood pressure in rats. *Eur. J. Pharmacol.* **877**, 173086. https://doi.org/10.1016/j.ejphar.2020.173086 (2020).
53. Luu, M. et al. The short-chain fatty acid pentanoate suppresses autoimmunity by modulating the metabolic-epigenetic crosstalk in lymphocytes. *Nat. Commun.* **10**, 760. https://doi.org/10.1038/s41467-019-08711-2 (2019).
54. Koeth, R. A. et al. Intestinal microbiota metabolism of L-carnitine, a nutrient in red meat, promotes atherosclerosis. *Nat. Med.* **19**, 576–585. https://doi.org/10.1038/nm.3145 (2013).
55. Velasquez, M. T., Ramezani, A., Manal, A. & Raj, D. S. Trimethylamine N-oxide: the good, the bad and the unknown. *Toxins (Basel)* **8**. https://doi.org/10.3390/toxins8110326 (2016).
56. Wen, Y. et al. Maternal serum trimethylamine-N-oxide is significantly increased in cases with established preeclampsia. *Pregnancy Hypertens.* **15**, 114–117. https://doi.org/10.1016/j.preghy.2018.12.001 (2019).
57. Chen, H., Li, J., Li, N., Liu, H. & Tang, J. Increased circulating trimethylamine N-oxide plays a contributory role in the development of endothelial dysfunction and hypertension in the RUPP rat model of preeclampsia. *Hypertens. Pregnancy* **38**, 96–104. https://doi.org/10.1080/10641955.2019.1584630 (2019).
58. Jaworska, K. et al. Hypertension in rats is associated with an increased permeability of the colon to TMA, a gut bacteria metabolite. *PLoS One* **12**, e0189310. https://doi.org/10.1371/journal.pone.0189310 (2017).
59. Ishimwe, J. A., Akinleye, A., Johnson, A. C., Garrett, M. R. & Sasser, J. M. Gestational gut microbial remodeling is impaired in a rat model of preeclampsia superimposed on chronic hypertension. *Physiol. Genomics* **53**, 125–136. https://doi.org/10.1152/physiolgenomics.00121.2020 (2021).
60. Tang, R. et al. The gut microbiota dysbiosis in preeclampsia contributed to trophoblast cell proliferation, invasion, and migration via lncRNA BC030099/NF-kappaB pathway. *Mediat. Inflamm.* **2022**, 6367264. https://doi.org/10.1155/2022/6367264 (2022).
61. Lopez-Tello, J. et al. Maternal gut microbiota Bifidobacterium promotes placental morphogenesis, nutrient transport and fetal growth in mice. *Cell. Mol. Life Sci.* **79**, 386. https://doi.org/10.1007/s00018-022-04379-y (2022).
62. Bankhead, P. et al. QuPath: Open source software for digital pathology image analysis. *Sci. Rep.* **7**, 16878. https://doi.org/10.1038/s41598-017-17204-5 (2017).
63. Kozich, J. J., Westcott, S. L., Baxter, N. T., Highlander, S. K. & Schloss, P. D. Development of a dual-index sequencing strategy and curation pipeline for analyzing amplicon sequence data on the MiSeq Illumina sequencing platform. *Appl. Environ. Microbiol.* **79**, 5112–5120. https://doi.org/10.1128/AEM.01043-13 (2013).
64. Schloss, P. D. et al. Introducing mothur: open-source, platform-independent, community-supported software for describing and comparing microbial communities. *Appl. Environ. Microbiol.* **75**, 7537–7541. https://doi.org/10.1128/AEM.01541-09 (2009).
65. Huse, S. M., Welch, D. M., Morrison, H. G. & Sogin, M. L. Ironing out the wrinkles in the rare biosphere through improved OTU clustering. *Environ. Microbiol.* **12**, 1889–1898. https://doi.org/10.1111/j.1462-2920.2010.02193.x (2010).
66. Edgar, R. C. UCHIME2: improved chimera prediction for amplicon sequencing. *bioRxiv* 074252. https://doi.org/10.1101/074252 (2016).
67. Westcott, S. L. & Schloss, P. D. OptiClust, an improved method for assigning amplicon-based sequence data to operational taxonomic Units. *mSphere* **2**. https://doi.org/10.1128/mSphereDirect.00073-17 (2017).
68. McMurdie, P. J. & Holmes, S. phyloseq: an R package for reproducible interactive analysis and graphics of microbiome census data. *PLoS One* **8**, e61217. https://doi.org/10.1371/journal.pone.0061217 (2013).
69. Love, M. I., Huber, W. & Anders, S. Moderated estimation of fold change and dispersion for RNA-seq data with DESeq2. *Genome Biol.* **15**, 550. https://doi.org/10.1186/s13059-014-0550-8 (2014).
70. Wickham, H. *ggplot2: Elegant Graphics for Data Analysis* (Springer International Publishing, 2016).

Acknowledgements

We thank the staff at the animal research facility of Laboratorio de Medicina Experimental for their excellent animal work. This work was supported by Charité Universitätsmedizin Berlin and Agencia Nacional de Promoción de la Investigación, el Desarrollo Tecnológico y la Innovación (Agencia I+D+I, grant number: PICT-2020-03263). Figure 1a was created with Biorender (http://www.biorender.com).

Author contributions

MMA analyzed and interpreted the microbiome data in Figs. 2, 3, 4, MSL and SIG conducted experiments and analyzed data for Fig. 1, GB designed and conducted animal experiments, HH provided funding and assisted

with SCFA analysis, RGG and FBF assisted with bioinformatics analyses, MLC and GB conceived the study, provided funding, supervised the research program and wrote the paper. All authors reviewed and approved the submitted version of the manuscript.

Declarations

Competing interests

The authors declare no competing interests.

Additional information

Correspondence and requests for materials should be addressed to G.B.

Reprints and permissions information is available at www.nature.com/reprints.

Publisher's note Springer Nature remains neutral with regard to jurisdictional claims in published maps and institutional affiliations.